



Article

Alterations in β -Cell Sphingolipid Profile Associated with ER Stress and iPLA₂ β : Another Contributor to β -Cell Apoptosis in Type 1 Diabetes

Tomader Ali ^{1,†} , Xiaoyong Lei ^{2,†}, Suzanne E. Barbour ³, Akio Koizumi ⁴, Charles E. Chalfant ⁵ and Sasanka Ramanadham ^{2,*} 

¹ Research Department, Imperial College London Diabetes Center, Abu Dhabi 51133, United Arab Emirates; tomader.ali@gmail.com

² Department of Cell, Developmental, and Integrative Biology and Comprehensive Diabetes Center, University of Alabama at Birmingham, Birmingham, AL 35294, USA; xlei@uab.edu

³ Department of Biochemistry and Biophysics, University of North Carolina at Chapel Hill, Chapel Hill, NC 27599, USA; barbours@email.unc.edu

⁴ Department of Health and Environmental Sciences, Kyoto Graduate School of Medicine, Kyoto 606-8501, Japan; koizumi@kyoto-hokenkai.or.jp

⁵ Department of Cell Biology, Microbiology and Molecular Biology, University of South Florida, Tampa, FL 33620, USA; cechalfant@usf.edu

* Correspondence: sramvem@uab.edu; Tel.: +1-205-996-5973; Fax: +1-205-996-5220

† These authors contributed equally to this work.



Citation: Ali, T.; Lei, X.; Barbour, S.E.; Koizumi, A.; Chalfant, C.E.; Ramanadham, S. Alterations in β -Cell Sphingolipid Profile Associated with ER Stress and iPLA₂ β : Another Contributor to β -Cell Apoptosis in Type 1 Diabetes. *Molecules* **2021**, *26*, 6361. <https://doi.org/10.3390/molecules26216361>

Academic Editor: Maurizio Battino

Received: 29 July 2021

Accepted: 11 October 2021

Published: 21 October 2021

Publisher's Note: MDPI stays neutral with regard to jurisdictional claims in published maps and institutional affiliations.



Copyright: © 2021 by the authors. Licensee MDPI, Basel, Switzerland. This article is an open access article distributed under the terms and conditions of the Creative Commons Attribution (CC BY) license (<https://creativecommons.org/licenses/by/4.0/>).

Abstract: Type 1 diabetes (T1D) development, in part, is due to ER stress-induced β -cell apoptosis. Activation of the Ca²⁺-independent phospholipase A₂ beta (iPLA₂ β) leads to the generation of pro-inflammatory eicosanoids, which contribute to β -cell death and T1D. ER stress induces iPLA₂ β -mediated generation of pro-apoptotic ceramides via neutral sphingomyelinase (NSMase). To gain a better understanding of the impact of iPLA₂ β on sphingolipids (SLs), we characterized their profile in β -cells undergoing ER stress. ESI/MS/MS analyses followed by ANOVA/Student's *t*-test were used to assess differences in sphingolipids molecular species in Vector (V) control and iPLA₂ β -overexpressing (OE) INS-1 and Akita (AK, spontaneous model of ER stress) and WT-littermate (AK-WT) β -cells. As expected, iPLA₂ β induction was greater in the OE and AK cells in comparison with V and WT cells. We report here that ER stress led to elevations in pro-apoptotic and decreases in pro-survival sphingolipids and that the inactivation of iPLA₂ β restores the sphingolipid species toward those that promote cell survival. In view of our recent finding that the SL profile in macrophages—the initiators of autoimmune responses leading to T1D—is not significantly altered during T1D development, we posit that the iPLA₂ β -mediated shift in the β -cell sphingolipid profile is an important contributor to β -cell death associated with T1D.

Keywords: phospholipase A₂; sphingolipids; diabetes; apoptosis

1. Introduction

Diabetes is a consequence of pancreatic islet β -cell dysfunction and/or reduced peripheral insulin sensitivity, and both type 1 and type 2 diabetes (T1D and T2D) are associated with β -cell apoptosis [1,2]. Therefore, it is important to elucidate the underlying involved mechanisms so that treatment regimens can be developed to protect the β -cells and prevent or delay diabetes development.

In addition to the extrinsic (receptor-mediated) and intrinsic (mitochondrial) apoptotic pathways, ER stress is recognized as an inducer of apoptosis in several disease states, including diabetes [3]. Reports from both experimental models and clinical settings have linked diabetes development with ER stress-induced β -cell apoptosis [4], and studies in our laboratory revealed an important role for the group VIA Ca²⁺-independent phospholipase

A₂ (iPLA₂β) in this process [5]. The iPLA₂s belong to a family of PLA₂s that include the secretory and cytosolic PLA₂s [6]. All of the PLA₂s catalyze the hydrolysis of the *sn*-2 substituent from membrane glycerophospholipids [7] to release a free fatty acid and a lysophospholipid. The cytosol-associated iPLA₂β participates in membrane phospholipid remodeling, signal transduction, cell proliferation, inflammation, and apoptosis [4,8,9]. Dysregulation of iPLA₂β has been associated with several neurodegenerative, skeletal, and vascular smooth muscle, bone formation, and cardiac disorders [4,9]. Other reports reveal there is also iPLA₂β induction in rodent models of T1D and human subjects with T1D [10–12].

Our examination of the link between iPLA₂β and ER stress revealed that β-cells undergoing thapsigargin-induced ER stress have increased expression of iPLA₂β and that inhibition of iPLA₂β by *S*-bromo-enol lactone (*S*-BEL), a select inhibitor of the β-isoform of iPLA₂ [13], significantly attenuates β-cell apoptosis [5,14,15]. Consistent with a role for iPLA₂β in this process, susceptibility to ER stress-induced apoptosis is amplified in INS-1 insulinoma cells overexpressing iPLA₂β [5] or in islet β-cells from RIP-iPLA₂β-Tg mice in which iPLA₂β is selectively overexpressed only in the β-cells [15]. In contrast, the knockdown [16] or knockout [15] of iPLA₂β reduced ER stress-induced β-cell apoptosis. Unexpectedly, in addition to its impact on iPLA₂β, ER stress promoted accumulations in ceramides, not via the *de novo* pathway, but via the increased hydrolysis of sphingomyelins by neutral sphingomyelinase 2 (NSMase2) [17]. In turn, the ceramides served to trigger mitochondrial apoptotic pathways, resulting in β-cell apoptosis [18].

While eicosanoids have been the main focus in studies of β-cell death [19–23], the contribution of sphingolipids to this process are less-well characterized. Ceramides are complex pro-apoptotic lipids, and it has been long recognized that sphingomyelin-derived ceramides play important roles in decreasing cell proliferation and increasing apoptosis [24–30]. Recently, there has been a tremendous increase in interest in sphingolipid biology, and various sphingolipid derivatives have been identified as bioactive molecules [31,32] with important roles in cell signaling [33–45]. The intriguingly diverse and dynamic manner in which sphingolipids interact with one another [42] emphasizes not only how intricate the sphingolipid family is and how much still remains unknown but more importantly, the therapeutic potential of targeting the regulation of sphingolipid-generating pathways. Therefore, we considered the possibility of whether there were widespread changes in sphingolipids metabolism due to iPLA₂β activation or due to ER stress in β-cells.

We used two β-cell models for our assessments: rat-derived INS-1 cells, genetically modified to overexpress iPLA₂β, where ER stress was induced with thapsigargin, and mouse-derived Akita cells, which is a spontaneous model of ER stress. The Akita mouse, due to a mutation in *Ins2* gene, accumulates misfolded proinsulin in the ER, leading to the development of ER stress in β-cells. Prolonged ER stress promotes β-cell apoptosis, leading to hyperglycemia and diabetes in the Akita mouse within a few weeks after birth [46]. β-cell lines derived from the Akita mouse exhibit an analogous spontaneous ER stress and a higher incidence of apoptosis, relative to β-cells derived from wild-type (WT) mice [16]. Utilizing mass spectrometry protocols, we report for the first time that ER stress leads to iPLA₂β-mediated differential distribution of sphingolipids, favoring the generation of pro-over anti-apoptotic sphingolipids, in β-cells. These data highlight a pivotal role for iPLA₂β in modulating sphingolipids profile in β-cells, and as a consequence, their survival.

2. Results

2.1. Altered iPLA₂β Expression, Chemical ER Stress Induction, and INS-1 Cell Sphingolipids

2.1.1. Verification of the INS-1 Cell Model

Initially, it was important to validate the INS-1 model for subsequent studies and immunoblotting and RT-qPCR analyses were performed to achieve this. Empty vector (V) cells cultured in the absence or presence of thapsigargin (T) were compared with iPLA₂β-overexpressing (OE) cells. Under basal conditions, the expression of GRP78 (Figure 1A),

the master regulator of the unfolded protein response to ER stress [47], iPLA₂β (Figure 1B) and NSMase (Figure 1C), was higher in the OE cells relative to V cells. Treatment with T led to the induction of all three in the V cells (VT), relative to untreated vector (V) cells. These findings confirm the (a) iPLA₂β phenotype of V and OE cells, (b) expression of higher NSMase2 and ER stress induction in the iPLA₂β OE cells, and (c) induction of ER stress, iPLA₂β, and NSMase2 in V cells by thapsigargin under conditions to be used for the following sphingolipids analyses. Furthermore, the results reveal the comparable induction of ER marker GRP78 and NSMase2 enzyme by the chemical stressor (T) and overexpression of iPLA₂β (in OE cells).

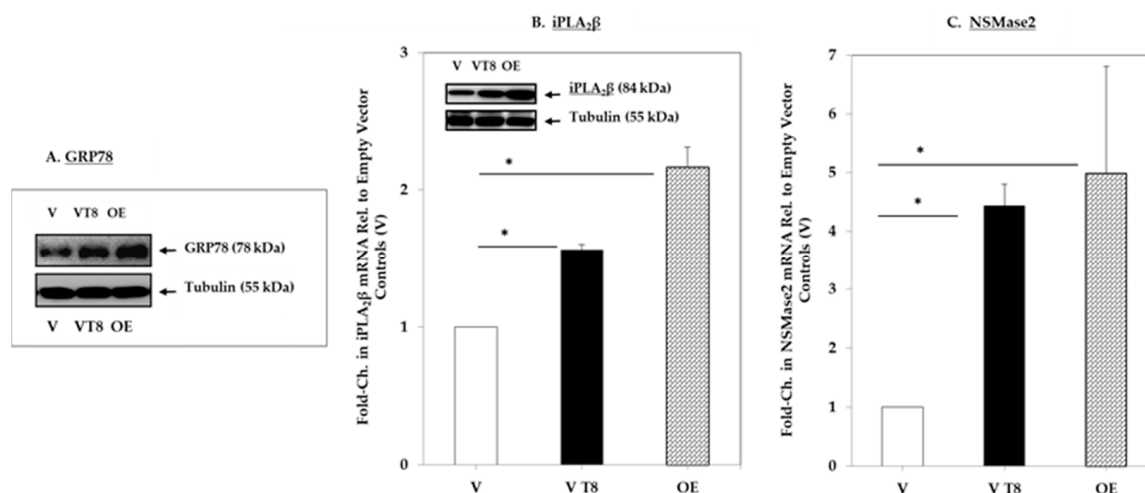


Figure 1. GRP78, iPLA₂β, and NSMase2 expression in INS-1 cells in the absence and presence of thapsigargin (T). Protein and cDNA were prepared from empty vector (V) INS-1 cells treated with DMSO (V) or thapsigargin (1 μM for 8 h (VT8)) and iPLA₂β-overexpressing (OE) INS-1 cells for immunoblotting and RT-qPCR analyses, respectively. Tubulin was used as a loading control in the protein analyses. (A,B). RT-qPCRs: 18S served as internal control, and fold-change in mRNA was calculated using the delta C_T method (ΔC_T) and expressed relative to V controls: (A) ER stress marker GRP78, (B) iPLA₂β mRNA (inset, iPLA₂β protein); and (C) NSMase2 mRNA. Data are presented as mean ± SEM, n = 3 per group. (* Significantly different from V control, p < 0.05).

2.1.2. Sphingolipids Profiles in INS-1 Cells

Next, LC-ESI/MS/MS analyses were used to assess the abundances of ceramide, sphingomyelin, monohexosyl ceramide (MHC), ceramide-1-phosphate (C1P), and sphingosine (So) and sphingosine-1-phosphate (So1P) molecular species (Appendix A) under conditions that increase iPLA₂β (OE and VT) cells compared to control (V) cells, as illustrated in Figure 2.

Ceramide molecular species were increased in the OE cells relative to V cells, as reflected by the higher pool of ceramides in the OE cells (Figure 2A). The induction of ER stress in V cells also resulted in an increase in the ceramide pool (in the VT cells) relative to untreated controls (V cells). As NSMase hydrolyzes sphingomyelins to generate ceramides, we investigated whether the observed increase in the ceramide pool was accompanied by changes in sphingomyelins. Indeed, we found similar decreases in the total pool of sphingomyelins (Figure 2B) in both models of increased ER stress and iPLA₂β (OE and VT cells) relative to untreated controls (V cells).

Since ceramides can be converted to various sphingolipids that manifest opposite biological activity, we assessed their abundances in the various cell models. Following glycosylation, ceramides can form monohexosyl ceramides (MHCs) [48]. Here, we report an increase in the MHC pool in both the OE and VT groups relative to the V control cells (Figure 2C). Ceramides can also be phosphorylated to generate inflammatory C1P, which can activate cPLA₂α and lead to the hydrolysis of arachidonic acid and PGE₂ formation [49]. Similarly, it can be speculated that C1P activates iPLA₂β to generate lipid mediators that

serve to amplify β -cell apoptosis. However, we report that the C1P pools in OE and VT cells were not significantly different from the corresponding pool in the untreated V group (Figure 2D). Both non-phosphorylated and phosphorylated So and Sa sphingolipid species were decreased in the VT group relative to V (Figure 2E); however, they were all higher in the OE group relative to the VT group. Collectively, these findings suggest that in general, the increased expression of iPLA₂ β and NSMase2 (Figure 1) promotes alterations in the sphingolipids profile to favor the generation of lipids recognized to be detrimental and pro-apoptotic, and away from those that may be protective and anti-apoptotic.

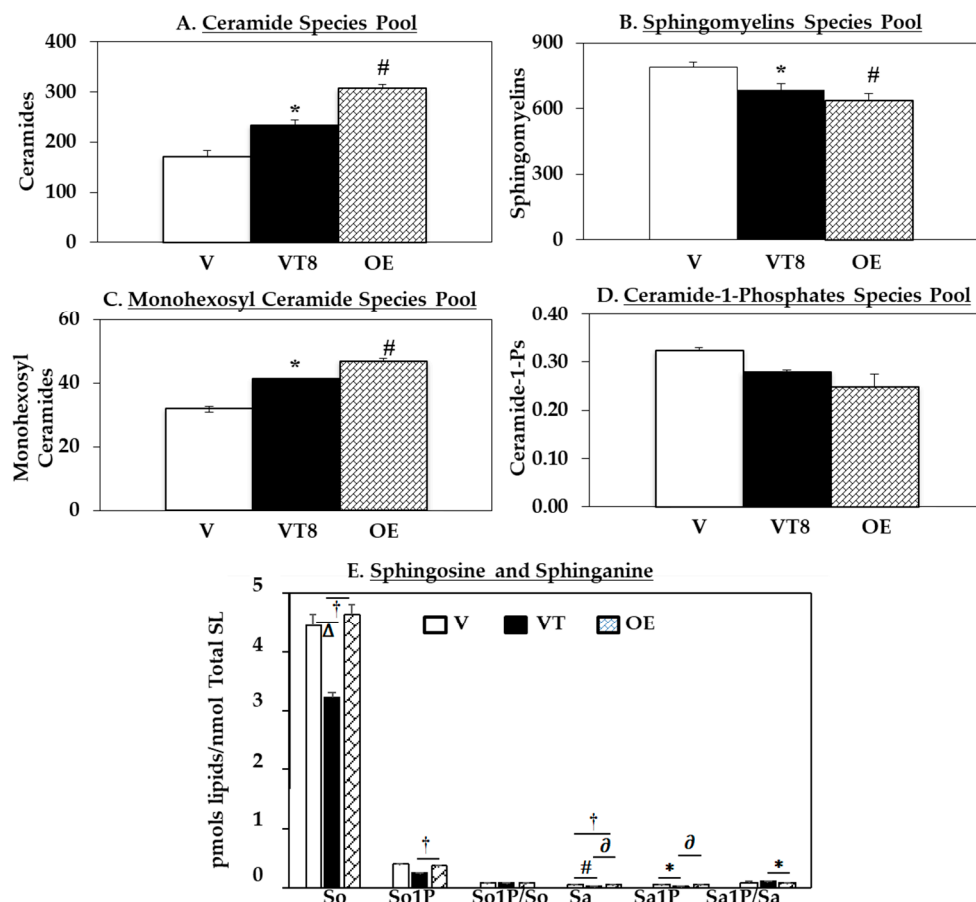


Figure 2. Sphingolipid (SL) abundances in INS-1 cells \pm ER stress. Lipids were extracted from empty vector INS-1 cells treated with DMSO (V) or thapsigargin (T, 1 μ M for 8 h, (VT8)) and iPLA₂ β -overexpressing (OE) INS-1 cells for LC ESI/MS/MS analyses: (A) Ceramide pool; (B) Sphingomyelin pool; (C) Monohexosyl ceramide pool; (D) Ceramide-1-phosphate pool; (E) Sphingosine and sphinganine. Data are presented as mean \pm SEM pmols lipid/nmol total sphingolipid). One-Way ANOVA was utilized for statistical analysis. (A–D), * OE group significantly different from V and # VT group significantly different from V; $p < 0.05$; (E), * $p < 0.05$, † $p < 0.01$, Δ $p < 0.005$, ∂ $p < 0.0005$, # $p < 0.0001$, $n = 3$ per group).

2.2. Spontaneous ER Stress Induction and β -Cell Sphingolipids

2.2.1. Verification of the Akita (AK) β -Cell Model

Since the above observations were made in INS-1 cells that were genetically modified to express higher iPLA₂ β or chemically induced (thapsigargin, T) to exhibit ER stress, we sought to examine whether spontaneous ER stress in β -cells promotes similar changes in the sphingolipids profile. The Akita β -cells, due to a spontaneous mutation in the *Ins2* gene that leads to the generation and accumulation of pre-proinsulin in the ER, develop spontaneous ER stress [50,51]. We previously demonstrated that this occurs in the Akita β -cells without chemical intervention [52]. Here, immunoblotting and qRT-PCR analyses confirm the induction of GRP78 (Figure 3A), which is associated with the higher expression of both iPLA₂ β (Figure 3A) and NSMase2 (Figure 3C) in the AK, relative to wild-type (WT)

cells. These analyses confirm that Akita cells, even under basal conditions, exhibit ER stress and that this is associated with higher $iPLA_2\beta$ and NSMase2.

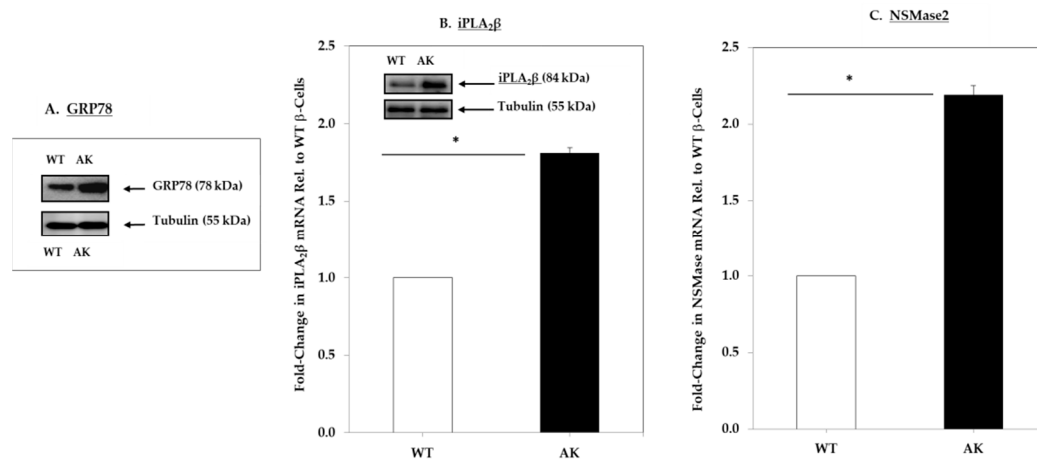


Figure 3. GRP78, $iPLA_2\beta$, and NSMase2 expression in wild-type (WT) and Akita (AK) β -cells. Protein and cDNA were prepared from WT control and AK and analyzed as in Figure 1: (A) ER stress marker GRP78 protein, (B) $iPLA_2\beta$ message, and protein (*inset*); (C) NSMase2 message. (* Significantly different from WT control, $p < 0.05$). Data are presented as mean \pm SEM, $n = 3$ per group.

2.2.2. Sphingolipids Profiles in WT and Akita (AK) β -Cells

Next, LC-ESI/MS/MS analyses, similar to the ones used with INS-1 cells, were performed to assess the relative abundances of sphingolipids (Appendix A) in the WT and AK cells (Figure 4). We report that associated with the spontaneous ER stress and higher basal $iPLA_2\beta$ levels, we observed increases in the pool of ceramides in the AK cells, relative to WT cells (Figure 4A). In view of the higher basal NSMase2, we examined for changes in sphingomyelins and found that the pool of sphingomyelin molecular species was decreased in the AK cells, relative to WT cells (Figure 4B). Further, the pools of MHC molecular species (Figure 4C) and the pro-apoptotic/inflammatory [53] C1P species (Figure 4D) were higher in the AK cells relative to WT cells. In general, the qualitative changes in AK cells were analogous to those described above in OE and VT cells, relative to untreated controls (V cells), reinforcing the suggestion that both $iPLA_2\beta$ increases and ER stress modify the sphingolipids profile to favor pro-apoptotic species in β -cells.

2.2.3. Effects of Inactivating $iPLA_2\beta$ on the Sphingolipids Profile in Akita (AK) β -Cells

As the changes in sphingolipids described in INS-1 and AK β -cells correlated with increased $iPLA_2\beta$, we examined whether they could be reversed by the inactivation of $iPLA_2\beta$. Further, because basal $iPLA_2\beta$ expression is higher in AK cells and they exhibit spontaneous ER stress, we examined the effects of S-BEL in AK cells in the absence and presence of thapsigargin (T). We find that both $iPLA_2\beta$ (Figure 5A) and NSMase2 (Figure 5B) are induced in the presence of thapsigargin (T), in both WTT and AKT cells, relative to WT and AK control cells, respectively.

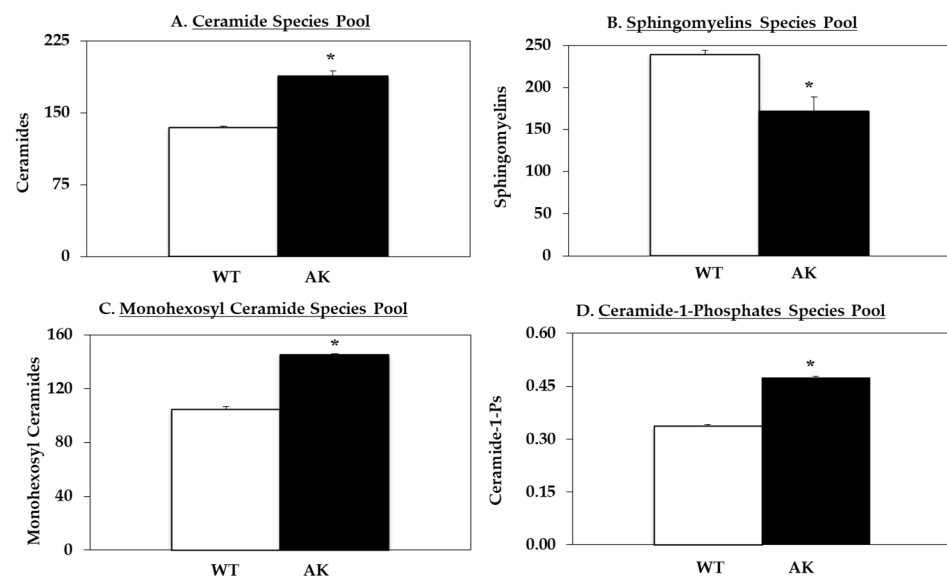


Figure 4. Basal sphingolipid (SL) abundances in WT and Akita β -cells. Lipids were extracted from empty WT and Akita β -cells for LC ESI/MS/MS analyses: (A) Ceramide pool; (B) Sphingomyelin pool; (C) Monohexosyl ceramide pool; (D) Ceramide-1-phosphate pool. Data are presented as mean \pm SEM pmols lipid/nmol total sphingolipid). (* Significantly different from WT control, $p < 0.05$, $n = 3$ per group).

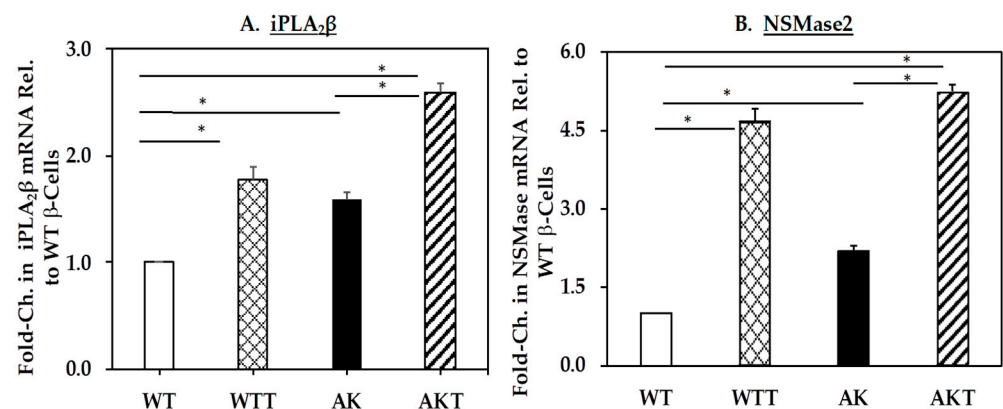


Figure 5. *iPLA₂ β* and *NSMase* expression \pm thapsigargin. mRNA was determined and quantified as described in Figure 1 and expressed relative to WT controls: (A) *iPLA₂ β* mRNA; and (B) *NSMase2* mRNA. (* Groups significantly different, $p < 0.05$) Data are presented as mean \pm SEM, $n = 3$ per group.

We next assessed the effects of chemical inhibition of *iPLA₂ β* by *S*-BEL on the sphingolipid profile in AK cells. The cells were pre-treated with *S*-BEL for 30 min prior to treatment with T. After 8 h, the cells were processed for sphingolipid analyses, as above, and the fold-change in sphingolipid species abundances in AKT cells relative to vehicle-treated cells (AK) was compared with those in AK cells treated with T + *S*-BEL (AKTB) relative to AKT. As expected, the ceramide molecular species were increased by thapsigargin (AKT/AK > 1, Figure 6A), but this effect was reversed by *S*-BEL (AKTB/AKT \leq 1) in all species except 18:1/24:0. Concurrently, thapsigargin-induced decreases in sphingomyelin molecular species (AKT/AK < 1, Figure 6B) were reversed by *S*-BEL. Similarly, various MHC species increased with thapsigargin (Figure 6C) were also decreased and reversed by *S*-BEL (AKTB/AKT \geq 1). However, the C1P species exhibited a differential regulation, where two species (18:1/16:0 and 18:1/24:0) were modestly decreased following thapsigargin treatment (AKT/AK > 1) but only 18:1/24:0 was rescued by *S*-BEL (AKTB/AKT > 1)

(Figure 6D). While no differences were evident in Sa or Sa1P among the groups, so was increased in the AK, relative to AKT, and the ratio of So1P/So decreased with S-BEL (AKTB).

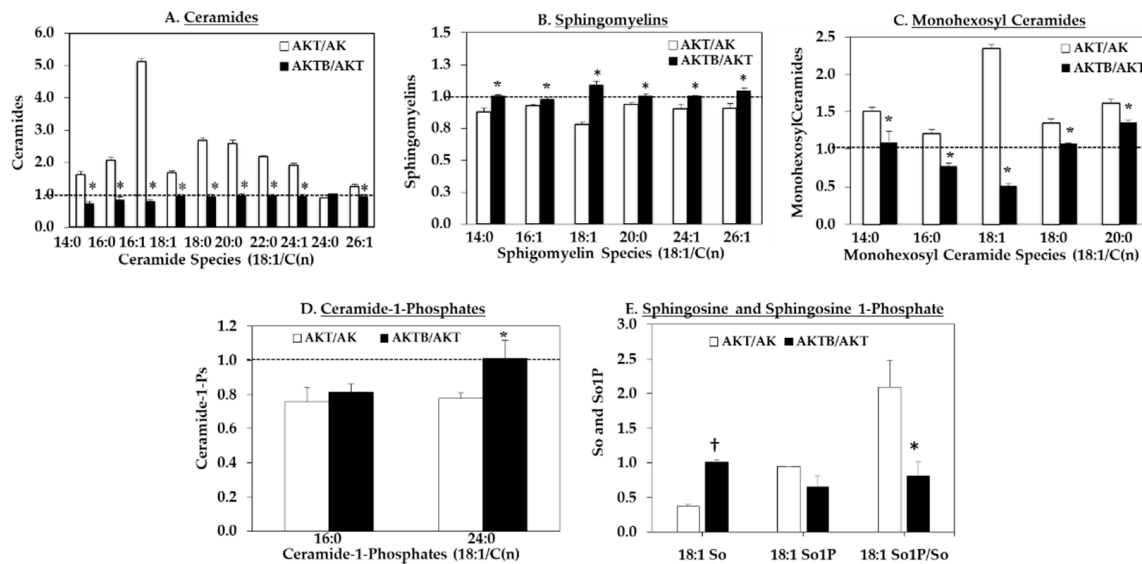


Figure 6. Effects of $iPLA_2\beta$ inhibition on sphingolipid abundances in Akita β -cells \pm ER stress. Lipids were extracted from Akita β -cells treated with thapsigargin (T, $1 \mu\text{M}$ for 8 h) in the absence and presence of S-BEL ($10 \mu\text{M}$). The ratio of sphingolipids \pm T (AKT/AT) and T \pm S-BEL (AKTB/AKT) are presented as mean \pm SEM pmols lipid/nmol total sphingolipid: (A) Ceramide pool; (B) Sphingomyelin pool; (C) Monohexosyl ceramide pool; (D) Ceramide-1-phosphate pool; and (E) Sphingosine (So) and So1P. Two-Way ANOVA was utilized for statistical analysis. (*,† Significantly different from AKT/AK; $p < 0.05$ and $p < 0.0005$, $n = 3$ per group).

3. Discussion

It has long been established that sphingolipids play important and dynamic roles in cellular physiology and that their levels are maintained under tightly regulated homeostasis processes via a variety of highly specialized enzymes [54–57]. We previously demonstrated that ER stress-mediated β -cell apoptosis is mediated, in part, through the activation of $iPLA_2\beta$ and that an increased expression of $iPLA_2\beta$ amplifies the susceptibility of β -cells to ER stress and subsequent β -cell apoptosis [4,5,8,16,17]. Increases in $iPLA_2\beta$ and ER stress were also associated with accumulations in ceramides, which contributed to β -cell death by triggering the intrinsic apoptotic pathway [4,18]. These observations provided evidence for the involvement of an $iPLA_2\beta$ /ceramide axis in promoting β -cell dysfunction and apoptosis, which are key contributors to the development of diabetes [1,2]. As reports from various experimental models and clinical settings suggested that ER stress contributes to β -cell apoptosis during the evolution of diabetes [4], we set out to assess the link between ER stress, $iPLA_2\beta$, and β -cell sphingolipids in the present study.

The roles of ceramides are related to their involvement in cell survival and are mainly considered to be pro-apoptotic [58–61]. Ceramide generation can occur through multiple pathways: (a) *de novo*, initiated by the condensation of serine and palmitoyl CoA, which is catalyzed by the rate-limiting enzyme serine palmitoyl transferase (SPT) [62]; (b) sphingomyelin hydrolysis by sphingomyelinases [48,63]; or (c) salvage pathway involving ceramidase [64]. Ceramides can be further converted to C1P by ceramide kinase or to MHCs by glucosylceramide synthase or ceramide galactosyl transferase [48]. Our work [14–18] indicates that the accumulation of ceramides during β -cell apoptosis due to ER stress occurs through the hydrolysis of sphingomyelins by NSMase2. Therefore, we aimed at determining whether the overall sphingolipid profile is modulated by $iPLA_2\beta$ in β -cells undergoing ER stress.

In the present study, MS protocols were applied to INS-1 cells and Akita β -cells to discern the impact of ER stress and iPLA₂ β expression on the abundances of various sphingolipids. The INS-1 cells are widely used in studies of β -cell function and survival and the availability in our laboratory of genetically modified iPLA₂ β -overexpressing (OE) INS-1 cells permitted examination of the effects of higher iPLA₂ β expression in the absence of chemically induced ER stress. In addition, parallel comparisons with thapsigargin-treated empty-vector (V) INS-1 cells enabled assessment of the effects of ER stress induction in the absence of genetic modification of iPLA₂ β expression. The Akita β -cells (AK) provided a model of spontaneous ER stress that also expresses higher basal iPLA₂ β [16], thus precluding consideration of the effects of chemical intervention or genetic modification.

Prior to the lipid analyses, immunoblotting and RT-PCR analyses confirmed (a) increased basal expression of iPLA₂ β , NSMase2, and GRP78 in the OE and AK cells, relative to V and WT cells, respectively and (b) induction of ER stress, iPLA₂ β , NSMase2, and GRP78 following exposure to thapsigargin in VT and AKT cells, relative to V and AK cells, respectively. Subsequently, LC-ESI/MS/MS analyses were used to identify molecular species of ceramides, sphingomyelins, monohexosyl ceramides (MHCs), ceramide-1-phosphate (C1P), sphinganine (Sa), sphingosine (So), and the So phosphate derivatives So1P.

Under basal conditions, comparisons of OE vs. V cells reveal that higher iPLA₂ β expression leads to (a) increases in the pro-apoptotic [65] ceramides, (b) decreases in anti-apoptotic [17] sphingomyelins, (c) increases in the primarily apoptotic [48] MHCs, (d) no change in inflammatory and apoptotic [66] C1P, and (e) no change in anti-apoptotic [53] So1P. Comparisons of VT vs. V cells following induction of ER stress, as reflected by increased expression of ER stress marker GRP78, and of iPLA₂ β in the VT cells revealed changes in VT sphingolipids that were similar to those in the OE cells.

Similar comparisons between the WT and AK cells under basal conditions revealed relative changes in the AK cells that mirrored those in the OE cells including (a) increases in ceramides, (b) decreases in sphingomyelins, (c) and increases in the MHCs. However, differences were noted in the C1P molecular species (unchanged in OE but increased in AK) and in the So1P/So ratio (unchanged in OE but increased in AKT). This is an important observation, as we also noted an increase in So1P/So ratio in the non-obese diabetic (NOD) mice, an autoimmune model of T1D [67]. The NOD mice develop insulinitis at 4–6 weeks of age and spontaneous T1D starting at 16–18 weeks of age [68]. β -Cell death and the development of T1D in the NOD is preceded by the induction of ER stress in the β -cells [69,70]. Given that So1P has been identified as a lipid that promotes T-cell migration and retention in inflamed tissues [71], it is likely that it could manifest deleterious effects in β -cells also.

Exposure to the ER stressor, thapsigargin, amplified the changes in the sphingolipids in AK cells, suggesting that ER stress and consequential downstream processes impact the sphingolipids profile. Since iPLA₂ β is also further induced, we considered the possibility that its activation contributes to the observed changes in sphingolipids. To assess this, AK cells were pre-treated with S-BEL prior to thapsigargin exposure, and this was found to reverse nearly all changes in the sphingolipids, with the exception of d18:1/16:0 C1P, toward control abundances. These findings are consistent with the involvement of iPLA₂ β activation in the regulation of β -cell sphingolipids.

While our data demonstrate similar modifications in the sphingolipids profile with higher iPLA₂ β and ER stress, differences were noted with respect to specific molecular species that were affected. Such discrepancies are not unexpected considering the inherent differences between the models studied, which include the (a) the high basal but long-term expression of iPLA₂ β in the iPLA₂ β -overexpressing INS-1 cells, which promotes ER stress vs. (b) the transient, short-term, chemically induced (thapsigargin) ER stress, which promotes iPLA₂ β expression in the Vector INS-1 cells vs. (c) the basal spontaneous and prolonged ER stress, which is associated with higher iPLA₂ β expression in the AK cells. In view of these differences, it is plausible that the sphingolipids-generating pathways are regulated dissimilarly, giving rise to variations in specific molecular species changes. Furthermore,

Scientific, Houston, TX, USA); Superscript III First-strand Synthesis System and Fast SYBR[®] Green PCR Master Mix, Roswell Park Memorial Institute (RPMI) 1640 medium, Dulbecco's modified Eagle's (DMEM) medium (Life Technologies Corporation, Grand Island, NY, USA); RNeasy kit (Qiagen Inc, Valencia, CA, USA); Group VIA iPLA₂β antibody T-14 (sc-14463), GRP78 (sc-1050), β-actin (sc-47778), and α-tubulin TU-02 (sc-8035) primary antibodies (Santa Cruz Biotechnology, Inc., Santa Cruz, CA, USA); thapsigargin (Sigma Co., St. Louis, MO, USA); LC/MS grade water, methanol and chloroform, formic acid and ammonium formate were purchased from (ThermoFisher-Scientific, Waltham, MA, USA); Phenomenex Kinetex 2.6 μm C18 100A 50 × 2.1 mm reverse phase HPLC chromatography column (Torrance, CA, USA); and disposable borosilicate glass culture tubes with PTFE-lined caps (VWR Laboratory Products, Westbury, NY, USA).

4.2. INS-1 Cell Culturing and Treatment

INS-1 (empty vector or iPLA₂β-overexpressing (OE)) cells were generated and cultured, as described [5]. Briefly, cells were cultured in RPMI 1640 medium, containing 11 mM glucose, 10% fetal calf serum, 10 mM HEPES buffer, 2 mM glutamine, 1 mM sodium pyruvate, 50 mM mercaptoethanol (BME), and 0.1% (*w/v*) each of penicillin and streptomycin in cell culture conditions (37 °C, 5%CO₂/95% air). Mouse Akita and WT β-cells were generated and cultured, as described [16,52,83]. Briefly, cells were cultured in DMEM medium containing 15% fetal calf serum, β-mercaptoethanol (150 μM), and 0.1% (*w/v*) each of penicillin and streptomycin in cell culture conditions (37 °C, 5%CO₂/95% air). For both cell lines, the medium was changed every other day, and the cells were passaged once a week. Thapsigargin (T) was prepared in DMSO and used at a final concentration of 1 μM. In some experiments, the cells were pre-treated for 30 min with the iPLA₂β inhibitor, S-BEL (10 μM). Then, the cells were washed prior to treatment with vehicle or thapsigargin. All experimental protocols included DMSO vehicle-only treated triplicate controls.

4.3. Quantitative Real-Time PCR

INS-1 cells (empty-Vector and OE) and WT and Akita β-cells were treated with DMSO alone or thapsigargin (1 μM) for 8 h. Total RNA was prepared using the RNeasy kit, and double-stranded cDNA was generated using the Superscript III First-strand Synthesis System kit, as described [14,15,17,18]. Real-time PCR was performed using Fast SYBR[®] Green PCR Master Mix and carried out in a plate-based LightCycler[®] 480 System (Roche Life Sciences). The primers were designed based on known sequences for iPLA₂β, NSMase2, and 18S, and the respective Gene Bank Gene ID numbers are as follows; Rat: #360426, #83537, and #100861533 and Mouse: #53357, #20598, and #18519791. Primer sets (sense/antisense) were as follows; Rat: iPLA₂β, tgtgacgtggacagcactagc/cccagaacgactatgga; NSMase, ccgatgcacactactcagaa/ggattgggtgtctggagaaca; and 18S, agtctgcctttgtacaca/gatccgaggcctcactaac and Mouse: iPLA₂β, agcttcaattcatgcagttcttggacgc/ttcgatcgggagatagcagcagctgg; NSMase, ccgatg-cacactactcagaa/ggattgggtgtctggagaaca; and 18S, agtctgcctttgtacaca/gatccgaggcctcactaac.

4.4. Immunoblotting

Cells were harvested following treatment and prepared for SDS-PAGE analyses, as described [5]. Briefly, harvested cells were washed once with PBS, sonicated, protein concentration was determined by the Bradford Protein Assay, and 30 μg of protein were analyzed on a 10% acrylamide SDS-PAGE gel. Resolved proteins were transferred onto Immobilon-P polyvinylidene difluoride (PVDF) membranes and probed (1°/2°) for iPLA₂β (1:500/1:1000), GRP78 (1:250/1:1000), and loading controls tubulin and actin both at (1:500/1:1000). Bands of interest were visualized by Universal Hood II Gel Imager (Bio-Rad) and densitometry analyses were carried out using the accompanying Image Lab software.

4.5. LC-Electrospray Ionization (ESI)-MS/MS Analyses of Sphingolipids

Cells were plated separately in 10 cm cell culture dishes to provide approximately 1×10^6 cells at harvesting. Following an 8 h treatment period with DMSO vehicle or thapsigargin, the cell culture dishes were placed on ice, washed twice with phosphate-buffered saline (PBS), and harvested by scraping in 200 μ L of PBS. The cells were immediately frozen and stored at -80 °C. At the time of analyses, the cells were thawed on ice followed by sonication to obtain a homogenous mixture, and lipids were extracted using a modified Bligh and Dyer method and analyzed, as described [84]. Briefly, to 200 μ L of the cells in PBS, 1.5 mL of 2:1 methanol/chloroform was added. The samples were spiked with internal standards consisting of 50 pmol each of d17:1 sphingosine, d17:0 sphinganine, d17:1 sphingosine-1-phosphate, d17:0 sphinganine-1-phosphate, d18:1/12:0 ceramide-1-phosphate, d18:1/12:0 sphingomyelin, d18:1/12:0 ceramide, and d18:1/12:0 monohexosyl ceramide. The mixture thus obtained was sonicated to disperse the cell clumps and incubated for 6 h at 48 °C. Following incubation, the samples were sonicated, followed by centrifugation to separate particulates. Then, the extracts were dried under vacuum and reconstituted by sonicating in 500 μ L of methanol followed by incubation at 48 °C for 15 min, vortexing, and incubation for an additional 15 min at 48 °C. Then, the samples were centrifuged to separate particulates, and 10 μ L was used for analysis. The lipids were separated using a Kinetix C18 column (50 \times 2.1 mm, 2.6 μ m) on a Nexera ultra-high-performance liquid chromatography system and eluted using a linear gradient (solvent A, 58:41:1 CH₃OH/water/HCOOH 5 mM ammonium formate; solvent B, 99:1 CH₃OH/HCOOH 5 mM ammonium formate, 20–100% B in 3.5 min and at 100% B for 4.5 min at a flow rate of 0.4 mL/min at 60 °C). Electrospray ionization (ESI) with tandem mass spectroscopy (MS/MS) on a 5500 QTRAP instrument was utilized for the detection and quantitation of analytes in the positive ion mode. Multiple reaction monitoring transitions utilized for the analytes are listed in Appendix A.

4.6. Statistical Analyses

Data were converted to mean \pm standard error of the means (SEMs), Student's *t*-test was applied to determine significant differences ($p < 0.05$) between two samples, and One-Way and Two-Way ANOVA statistical analyses were applied to determine significant differences (at $p < 0.05$) between more than two sample groups.

5. Conclusions

In summary, our data demonstrate for the first time that iPLA₂ β and ER stress in β -cells, in concert, modulate the sphingolipids profile in β -cells and that the consequential redistribution between the various sphingolipids favors apoptosis over the survival of the β -cells. To our knowledge, molecular species assessments of ceramide-derived sphingolipids have not been examined in detail in β -cells, and our findings provide the basis for future studies that will address important issues in a cell system where the dysregulation of sphingolipids generation could impact its survival, and as a consequence, could play a critical role in the evolution of diabetes or other inflammatory diseases [85,86].

Author Contributions: T.A., X.L. conceived and coordinated the study, performed experiments, analyzed data, and prepared the manuscript; S.E.B. contributed manuscript's data analyses; A.K. generated the Akita cells; C.E.C. performed the lipidomic analyses; and S.R. conceived and coordinated the study, analyzed data, contributed to preparation of the figures, and edited the paper. All authors have read and agreed to the published version of the manuscript.

Funding: This work was supported by grants from the National Institutes of Health (DK69455 and DK-110292 to SR) and the American Diabetes Association (SR); Veteran's Administration (VA Merit Award BX001792), Research Career Scientist Award, National Institutes of Health (HL072925 and CA154314, US-Israel Binational Science Foundation (BSF#2011380) to CEC; NH1C06-RR17393 (to Virginia Commonwealth University for renovation), NIH/NCI Cancer Center Support Grant P30 CA016059 (to Massey Cancer Center), a National Research Service Award-T32 Post-Doctoral

Fellowship in Wound Healing GM008695 (DSW) and a Career Development Award (CDA1) from the Department of Veterans Affairs (DSW).

Institutional Review Board Statement: Not applicable.

Informed Consent Statement: Not applicable.

Data Availability Statement: Not applicable.

Conflicts of Interest: The authors declare no conflict of interest.

Abbreviations

AK, Akita β -cells; C1P, ceramide-1-phosphatate; CM, ceramide; iPLA₂ β , cytosol-associated Ca²⁺-independent phospholipase A₂; MHC, monohexosyl ceramide; OE, iPLA₂ β -overexpressing INS-1 cells; NOD, non-obese diabetic, NSMase2, neutral sphingomyelinase 2; Sa, sphinganine; Sa1P, sphinganine-1-phosphate; SM, sphingomyelin; So, sphingosine; So1P, sphingosine-1-phosphate; PTFE, polytetrafluoroethylene; V, empty-vector INS-1 cells; and WT, wild-type β -cells.

Appendix A

Table A1. MRM Transitions monitored for the investigated sphingolipid species.

Species	Precursor Ion (<i>m/z</i>)	Product Ion (<i>m/z</i>)	DP	CE
d _{17:1} Sphingosine	286.4	268.3	120	15.0
d _{17:0} Sphinganine	288.4	270.4	120	21.0
d _{18:1} Sphingosine	300.5	282.3	120	21.0
d _{18:0} Sphinganine	302.5	284.3	120	21.0
d _{17:1} S1P	366.4	250.4	120	23.0
d _{17:0} Sa1P	368.4	252.4	120	23.0
d _{18:1} S1P	380.4	264.4	120	25.0
d _{18:0} Sa1P	382.4	266.4	120	25.0
d _{18:1/12:0} Ceramide	482.6	264.4	80.0	41.0
d _{18:1/12:0} C1P	562.4	264.4	80.0	41.0
d _{18:1/12:0} MonoHex	644.6	264.4	80.0	41.0
d _{18:1/12:0} SM	647.7	184.4	80.0	41.0
d _{18:1/14:0} Ceramide	510.7	264.4	80.0	43.5
d _{18:1/14:0} C1P	590.4	264.4	80.0	43.5
d _{18:1/14:0} MonoHex	672.6	264.4	80.0	43.5
d _{18:1/14:0} SM	675.7	184.4	80.0	43.5
d _{18:1/16:0} Ceramide	538.7	264.4	80.0	46.0
d _{18:1/16:0} C1P	618.5	264.4	80.0	46.0
d _{18:1/16:0} MonoHex	700.7	264.4	80.0	46.0
d _{18:1/16:0} SM	703.8	184.4	80.0	46.0
d _{18:0/16:0} Ceramide	540.7	266.4	80.0	46.0
d _{18:0/16:0} C1P	620.5	266.4	80.0	46.0
d _{18:0/16:0} MonoHex	702.5	266.4	80.0	46.0
d _{18:0/16:0} SM	705.8	184.4	80.0	46.0
d _{18:1/18:1} Ceramide	564.7	264.4	80.0	48.5
d _{18:1/18:1} C1P	644.5	264.4	80.0	48.5
d _{18:1/18:1} MonoHex	728.7	264.4	80.0	48.5
d _{18:1/18:1} SM	731.8	184.4	80.0	48.5
d _{18:1/18:0} Ceramide	566.7	264.4	80.0	48.5
d _{18:1/18:0} C1P	646.5	264.4	80.0	48.5
d _{18:1/18:0} MonoHex	730.7	264.4	80.0	48.5
d _{18:1/18:0} SM	733.8	184.4	80.0	48.5

Table A2. Cont.

d18:1/14:0	0.05	0.00	0.06	0.01	[∂] 0.08	0.00	0.03866	0.01027	0.04127	0.00461	0.03362	0.00457
d18:1/16:0	4.23	0.07	^Δ 4.97	0.06	[∂] 9.84	0.51	0.23508	0.03697	0.19329	0.04573	0.17544	0.04935
d18:0/16:0	1.85	0.16	^Δ 4.33	0.27	2.11	0.09	0.00393	0.00287	0.00113	0.00036	0.00308	0.00099
d18:1/18:1	0.07	0.01	* 0.05	0.00	[∂] 0.22	0.01	0.19495	0.07664	0.11587	0.06149	0.20923	0.13018
d18:1/18:0	1.86	0.08	^Δ 1.21	0.05	[∂] 3.83	0.11	0.05083	0.00469	0.05130	0.00176	0.04164	0.01235
d18:1/20:0	0.14	0.00	^Δ 0.11	0.00	# 0.26	0.00	0.00907	0.00317	0.00927	0.00361	0.00835	0.00351
d18:1/22:0	2.96	0.10	3.08	0.06	[∂] 4.48	0.11	0.03667	0.01250	0.04694	0.00929	0.02706	0.00633
d18:1/24:1	1.26	0.14	1.49	0.02	# 2.74	0.06	0.04243	0.01041	0.04558	0.00501	0.04003	0.00845
d18:1/24:0	25.29	0.73	^Δ 31.14	0.36	^Δ 34.12	0.82	0.30555	0.03705	0.57806	0.01633	0.23822	0.02777
d18:1/26:1	0.10	0.01	0.16	0.03	0.11	0.00	0.01189	0.00665	0.01646	0.00444	0.01715	0.00547
d18:1/26:0	0.56	0.02	^Δ 0.81	0.01	* 0.76	0.05	0.00721	0.00205	* 0.01152	0.00117	0.00902	0.00285

INS-1 cell sphingolipid molecular species. Mass spectrometry techniques were utilized to decipher ceramide species in INS-1 cells that contained empty iPLA₂β vector control cells (V), ER stress inducer thapsigargin (T) treated V cells (VT) and iPLA₂β-overexpressing cells (OEs). Ceramide species investigated included ceramides and sphingomyelins (PANEL A) and monohexosyl ceramide and ceramide-1-phosphates (PANEL B). Data are represented as SEM ± SE (*n* = 3 per group) with varied statistical significance from control V cells; * *p* < 0.05, † *p* < 0.01, ^Δ *p* < 0.005, [∂] *p* < 0.0005, # *p* < 0.0001.

References

- Tisch, R.; McDevitt, H. Insulin-dependent diabetes mellitus. *Cell* **1996**, *85*, 291–297. [[CrossRef](#)]
- Butler, A.E.; Janson, J.; Bonner-Weir, S.; Ritzel, R.; Rizza, R.A.; Butler, P.C. β-Cell deficit and increased β-cell apoptosis in humans with type 2 diabetes. *Diabetes* **2003**, *52*, 102–110. [[CrossRef](#)] [[PubMed](#)]
- Harding, H.P.; Zeng, H.; Zhang, Y.; Jungries, R.; Chung, P.; Plesken, H.; Sabatini, D.D.; Ron, D. Diabetes mellitus and exocrine pancreatic dysfunction in perk-/- mice reveals a role for translational control in secretory cell survival. *Mol. Cell* **2001**, *7*, 1153–1163. [[CrossRef](#)]
- Lei, X.; Zhang, S.; Emani, B.; Barbour, S.E.; Ramanadham, S. A link between endoplasmic reticulum stress-induced β-cell apoptosis and the group VIA Ca²⁺-independent phospholipase A2 (iPLA₂β). *Diabetes Obes. Metab.* **2010**, *12*, 93–98. [[CrossRef](#)] [[PubMed](#)]
- Ramanadham, S.; Hsu, F.; Zhang, S.; Jin, C.; Bohrer, A.; Song, H.; Bao, S.; Ma, Z.; Turk, J. Apoptosis of insulin-secreting cells induced by endoplasmic reticulum stress is amplified by overexpression of group VIA calcium-independent phospholipase A2 (iPLA₂β) and suppressed by inhibition of iPLA₂β. *Biochemistry* **2004**, *43*, 918–930. [[CrossRef](#)]
- Dennis, E.A.; Cao, J.; Hsu, Y.H.; Magrioti, V.; Kokotos, G. Phospholipase A2 enzymes: Physical structure, biological function, disease implication, chemical inhibition, and therapeutic intervention. *Chem. Rev.* **2011**, *111*, 6130–6185. [[CrossRef](#)] [[PubMed](#)]
- Gijón, M.A.; Leslie, C.C. Phospholipases A2. *Semin. Cell. Dev. Biol.* **1997**, *8*, 297–303. [[CrossRef](#)] [[PubMed](#)]
- Lei, X.; Barbour, S.E.; Ramanadham, S. Group VIA Ca²⁺-independent phospholipase A2 (iPLA₂β) and its role in beta-cell programmed cell death. *Biochimie* **2010**, *92*, 627–637. [[CrossRef](#)] [[PubMed](#)]
- Wilkins, W.P., 3rd; Barbour, S.E. Group VI phospholipases A2: Homeostatic phospholipases with significant potential as targets for novel therapeutics. *Curr. Drug Targets* **2008**, *9*, 683–697. [[CrossRef](#)]
- Ayilavarapu, S.; Kantarci, A.; Fredman, G.; Turkoglu, O.; Omori, K.; Liu, H.; Iwata, T.; Yagi, M.; Hasturk, H.; Van Dyke, T.E. Diabetes-Induced Oxidative Stress Is Mediated by Ca²⁺-Independent Phospholipase A2 in Neutrophils. *J. Immunol.* **2010**, *184*, 1507–1515. [[CrossRef](#)] [[PubMed](#)]
- Rahnema, P.; Shimoni, Y.; Nygren, A. Reduced conduction reserve in the diabetic rat heart: Role of iPLA₂ activation in the response to ischemia. *Am. J. Physiol. Circ. Physiol.* **2011**, *300*, H326–H334. [[CrossRef](#)]
- Xie, Z.; Gong, M.C.; Su, W.; Xie, D.; Turk, J.; Guo, Z. Role of Calcium-independent Phospholipase A₂β in High Glucose-induced Activation of RhoA, Rho Kinase, and CPI-17 in Cultured Vascular Smooth Muscle Cells and Vascular Smooth Muscle Hypercontractility in Diabetic Animals. *J. Biol. Chem.* **2010**, *285*, 8628–8638. [[CrossRef](#)]
- Jenkins, C.M.; Han, X.; Mancuso, D.J.; Gross, R.W. Identification of Calcium-independent Phospholipase A2 (iPLA₂) β, and Not iPLA₂γ, as the Mediator of Arginine Vasopressin-induced Arachidonic Acid Release in A-10 Smooth Muscle Cells. Enantioselective mechanism-based discrimination of mammalian iPLA₂s. *J. Biol. Chem.* **2002**, *277*, 32807–32814. [[CrossRef](#)] [[PubMed](#)]
- Lei, X.; Zhang, S.; Bohrer, A.; Barbour, S.E.; Ramanadham, S. Role of calcium-independent phospholipase A₂β in human pancreatic islet β-cell apoptosis. *Am. J. Physiol. Endocrinol. Metab.* **2012**, *303*, E1386–E1395. [[CrossRef](#)]
- Lei, X.; Bone, R.N.; Ali, T.; Wohltmann, M.; Gai, Y.; Goodwin, K.J.; Bohrer, A.E.; Turk, J.; Ramanadham, S. Genetic modulation of islet beta-cell iPLA₂β expression provides evidence for its impact on beta-cell apoptosis and autophagy. *Islets* **2013**, *5*, 29–44. [[CrossRef](#)] [[PubMed](#)]

16. Lei, X.; Zhang, S.; Barbour, S.E.; Bohrer, A.; Ford, E.L.; Koizumi, A.; Papa, F.R.; Ramanadham, S. Spontaneous development of endoplasmic reticulum stress that can lead to diabetes mellitus is associated with higher calcium-independent phospholipase A2 expression: A role for regulation by SREBP-1. *J. Biol. Chem.* **2010**, *285*, 6693–6705. [[CrossRef](#)]
17. Lei, X.; Zhang, S.; Bohrer, A.; Bao, S.; Song, H.; Ramanadham, S. The group VIA calcium-independent phospholipase A2 participates in ER stress-induced INS-1 insulinoma cell apoptosis by promoting ceramide generation via hydrolysis of sphingomyelins by neutral sphingomyelinase. *Biochemistry* **2007**, *46*, 10170–10185. [[CrossRef](#)]
18. Lei, X.; Zhang, S.; Bohrer, A.; Ramanadham, S. Calcium-independent phospholipase A2 (iPLA₂ beta)-mediated ceramide generation plays a key role in the cross-talk between the endoplasmic reticulum (ER) and mitochondria during ER stress-induced insulin-secreting cell apoptosis. *J. Biol. Chem.* **2008**, *283*, 34819–34832. [[CrossRef](#)]
19. Inceoglu, B.; Bettaieb, A.; Haj, F.G.; Gomes, A.V.; Hammock, B.D. Modulation of mitochondrial dysfunction and endoplasmic reticulum stress are key mechanisms for the wide-ranging actions of epoxy fatty acids and soluble epoxide hydrolase inhibitors. *Prostaglandins Other Lipid Mediat.* **2017**, *133*, 68–78. [[CrossRef](#)]
20. Jung, T.W.; Hwang, H.-J.; Hong, H.C.; Choi, H.Y.; Yoo, H.J.; Baik, S.H.; Choi, K.M. Resolvin D1 reduces ER stress-induced apoptosis and triglyceride accumulation through JNK pathway in HepG2 cells. *Mol. Cell. Endocrinol.* **2014**, *391*, 30–40. [[CrossRef](#)] [[PubMed](#)]
21. Luo, P.; Wang, M.H. Eicosanoids, beta-cell function, and diabetes. *Prostaglandins Other Lipid Mediat.* **2011**, *95*, 1–10. [[CrossRef](#)]
22. Ma, K.; Nunemaker, C.S.; Wu, R.; Chakrabarti, S.K.; Taylor-Fishwick, D.A.; Nadler, J.L. 12-Lipoxygenase Products Reduce Insulin Secretion and β -Cell Viability in Human Islets. *J. Clin. Endocrinol. Metab.* **2010**, *95*, 887–893. [[CrossRef](#)] [[PubMed](#)]
23. McDuffie, M.; Maybee, N.A.; Keller, S.R.; Stevens, B.K.; Garmey, J.C.; Morris, M.A.; Kropf, E.; Rival, C.; Ma, K.; Carter, J.D.; et al. Nonobese diabetic (NOD) mice congenic for a targeted deletion of 12/15-lipoxygenase are protected from autoimmune diabetes. *Diabetes* **2008**, *57*, 199–208. [[CrossRef](#)] [[PubMed](#)]
24. Hannun, Y.A. Functions of Ceramide in Coordinating Cellular Responses to Stress. *Science* **1996**, *274*, 1855–1859. [[CrossRef](#)] [[PubMed](#)]
25. Obeid, L.M.; Linardic, C.M.; Karolak, L.A.; Hannun, Y.A. Programmed Cell Death Induced by Ceramide. *Science* **1993**, *259*, 1769–1771. [[CrossRef](#)]
26. Testi, R. Sphingomyelin breakdown and cell fate. *Trends Biochem. Sci.* **1996**, *21*, 468–471. [[CrossRef](#)]
27. Verheij, M.; Bose, R.; Lin, X.H.; Yao, B.; Jarvis, W.D.; Grant, S.L.; Birrer, M.J.; Szabo, E.; Zon, L.I.; Kyriakis, J.M.; et al. Requirement for ceramide-initiated SAPK/JNK signalling in stress-induced apoptosis. *Nature* **1996**, *380*, 75–79. [[CrossRef](#)]
28. Tuzcu, H.; Unal, B.; Kirac, E.; Konuk, E.; Ozcan, F.; Elpek, G.; Demir, N.; Aslan, M. Neutral sphingomyelinase inhibition alleviates apoptosis, but not ER stress, in liver ischemia–reperfusion injury. *Free Radic. Res.* **2017**, *51*, 253–268. [[CrossRef](#)]
29. Garcia-Ruiz, C.; Morales, A.; Fernández-Checa, J.C. Glycosphingolipids and cell death: One aim, many ways. *Apoptosis* **2015**, *20*, 607–620. [[CrossRef](#)]
30. Boslem, E.; Weir, J.M.; MacIntosh, G.; Sue, N.; Cantley, J.; Meikle, P.J.; Biden, T.J. Alteration of endoplasmic reticulum lipid rafts contributes to lipotoxicity in pancreatic beta-cells. *J. Biol. Chem.* **2013**, *288*, 26569–26582. [[CrossRef](#)]
31. Bartke, N.; Hannun, Y.A. Bioactive sphingolipids: Metabolism and function. *J. Lipid Res.* **2009**, *50*, S91–S96. [[CrossRef](#)]
32. Canals, D.; Perry, D.M.; Jenkins, R.W.; Hannun, Y.A. Drug targeting of sphingolipid metabolism: Sphingomyelinases and ceramidases. *Br. J. Pharmacol.* **2011**, *163*, 694–712. [[CrossRef](#)]
33. Hannun, Y.A.; Obeid, L.M. Principles of bioactive lipid signalling: Lessons from sphingolipids. *Nat. Rev. Mol. Cell Biol.* **2008**, *9*, 139–150. [[CrossRef](#)]
34. Gault, C.R.; Obeid, L.M.; Hannun, Y.A. An overview of sphingolipid metabolism: From synthesis to breakdown. *Adv. Exp. Med. Biol.* **2010**, *688*, 1–23.
35. Albeituni, S.; Stiban, J. Roles of Ceramides and Other Sphingolipids in Immune Cell Function and Inflammation. *Adv. Exp. Med. Biol.* **2019**, *1161*, 169–191. [[CrossRef](#)] [[PubMed](#)]
36. Fugio, L.B.; Coeli-Lacchini, F.; Leopoldino, A.M. Sphingolipids and Mitochondrial Dynamic. *Cells* **2020**, *9*, 581. [[CrossRef](#)]
37. Gomez-Larrauri, A.; Presa, N.; Dominguez-Herrera, A.; Ouro, A.; Trueba, M.; Gomez-Muñoz, A. Role of bioactive sphingolipids in physiology and pathology. *Essays Biochem.* **2020**, *64*, 579–589. [[CrossRef](#)] [[PubMed](#)]
38. Hannun, Y.A.; Obeid, L.M. Sphingolipids and their metabolism in physiology and disease. *Nat. Rev. Mol. Cell Biol.* **2018**, *19*, 175–191. [[CrossRef](#)] [[PubMed](#)]
39. Tan-Chen, S.; Guitton, J.; Bourron, O.; Le Stunff, H.; Hajdich, E. Sphingolipid Metabolism and Signaling in Skeletal Muscle: From Physiology to Physiopathology. *Front. Endocrinol.* **2020**, *11*, 491. [[CrossRef](#)]
40. Trayssac, M.; Hannun, Y.A.; Obeid, L.M. Role of sphingolipids in senescence: Implication in aging and age-related diseases. *J. Clin. Investig.* **2018**, *128*, 2702–2712. [[CrossRef](#)]
41. Young, S.A.; Mina, J.G.; Denny, P.W.; Smith, T.K. Sphingolipid and Ceramide Homeostasis: Potential Therapeutic Targets. *Biochem. Res. Int.* **2012**, *2012*, 248135. [[CrossRef](#)] [[PubMed](#)]
42. Mullen, T.D.; Jenkins, R.W.; Clarke, C.J.; Bielawski, J.; Hannun, Y.A.; Obeid, L.M. Ceramide synthase-dependent ceramide generation and programmed cell death: Involvement of salvage pathway in regulating postmitochondrial events. *J. Biol. Chem.* **2011**, *286*, 15929–15942. [[CrossRef](#)] [[PubMed](#)]

43. Hou, Q.; Jin, J.; Zhou, H.; Novgorodov, S.A.; Bielawska, A.; Szulc, Z.M.; Hannun, Y.A.; Obeid, L.M.; Hsu, Y.T. Mitochondrially targeted ceramides preferentially promote autophagy, retard cell growth, and induce apoptosis. *J. Lipid Res.* **2011**, *52*, 278–288. [[CrossRef](#)] [[PubMed](#)]
44. Young, M.; Kester, M.; Wang, H.-G. Sphingolipids: Regulators of crosstalk between apoptosis and autophagy. *J. Lipid Res.* **2013**, *54*, 5–19. [[CrossRef](#)]
45. Kim, Y.M.; Park, T.S.; Kim, S.G. The role of sphingolipids in drug metabolism and transport. *Expert Opin. Drug Metab. Toxicol.* **2013**, *9*, 319–331. [[CrossRef](#)]
46. Oyadomari, S.; Koizumi, A.; Takeda, K.; Gotoh, T.; Akira, S.; Araki, E.; Mori, M. Targeted disruption of the Chop gene delays endoplasmic reticulum stress-mediated diabetes. *J. Clin. Investig.* **2002**, *109*, 525–532. [[CrossRef](#)]
47. Ni, M.; Lee, A.S. ER chaperones in mammalian development and human diseases. *FEBS Lett.* **2007**, *581*, 3641–3651. [[CrossRef](#)]
48. Boslem, E.; Meikle, P.J.; Biden, T.J. Roles of ceramide and sphingolipids in pancreatic beta-cell function and dysfunction. *Islets* **2012**, *4*, 177–187. [[CrossRef](#)]
49. Simanshu, D.; Kamlekar, R.; Wijesinghe, D.S.; Zou, X.; Zhai, X.; Mishra, S.; Molotkovsky, J.G.; Malinina, L.; Hinchcliffe, E.H.; Chalfant, C.E.; et al. Non-vesicular trafficking by a ceramide-1-phosphate transfer protein regulates eicosanoids. *Nature* **2013**, *500*, 463–467. [[CrossRef](#)]
50. Kayo, T.; Koizumi, A. Mapping of murine diabetogenic gene mody on chromosome 7 at D7Mit258 and its involvement in pancreatic islet and beta cell development during the perinatal period. *J. Clin. Investig.* **1998**, *101*, 2112–2118. [[CrossRef](#)]
51. Yoshioka, M.; Kayo, T.; Ikeda, T.; Koizumi, A. A novel locus, Mody4, distal to D7Mit189 on chromosome 7 determines early-onset NIDDM in nonobese C57BL/6 (Akita) mutant mice. *Diabetes* **1997**, *46*, 887–894. [[CrossRef](#)]
52. Barbour, S.E.; Nguyen, P.T.; Park, M.; Emani, B.; Lei, X.; Kambalapalli, M.; Ramanadham, S. Group VIA Phospholipase A2 (iPLA2 β) Modulates Bcl-x 5'-Splice Site Selection and Suppresses Anti-apoptotic Bcl-x(L) in β -Cells. *J. Biol. Chem.* **2015**, *290*, 11021–11031. [[CrossRef](#)]
53. Adada, M.M.; Orr-Gandy, K.A.; Snider, A.J.; Canals, D.; Hannun, Y.A.; Obeid, L.M.; Clarke, C.J. Sphingosine kinase 1 regulates tumor necrosis factor-mediated RANTES induction through p38 mitogen-activated protein kinase but independently of nuclear factor κ B activation. *J. Biol. Chem.* **2013**, *288*, 27667–27679. [[CrossRef](#)] [[PubMed](#)]
54. Obeid, L.M.; Hannun, Y.A. Ceramide, Stress, and a “LAG” in Aging. *Sci. Aging Knowl. Environ.* **2003**, *2003*, pe27. [[CrossRef](#)]
55. Mathias, S.; Kolesnick, R. Ceramide: A novel second messenger. *Adv. Lipid Res.* **1993**, *25*, 65–90.
56. Merrill, A.H. Ceramide: A new lipid “second messenger”? *Nutr. Rev.* **1992**, *50*, 78–80. [[CrossRef](#)]
57. Dobrowsky, R.T.; Hannun, Y. Ceramide-activated protein phosphatase: Partial purification and relationship to protein phosphatase 2A. *Adv. Lipid Res.* **1993**, *25*, 91–104.
58. Rego, A.; Costa, M.; Chaves, S.; Matmati, N.; Pereira, H.; Sousa, M.J.; Moradas-Ferreira, P.; Hannun, Y.A.; Costa, V.; Côte-Real, M. Modulation of Mitochondrial Outer Membrane Permeabilization and Apoptosis by Ceramide Metabolism. *PLoS ONE* **2012**, *7*, e48571. [[CrossRef](#)] [[PubMed](#)]
59. Hage-Sleiman, R.; Esmerian, M.O.; Kobeissy, H.; Dbaiibo, G. p53 and Ceramide as Collaborators in the Stress Response. *Int. J. Mol. Sci.* **2013**, *14*, 4982–5012. [[CrossRef](#)] [[PubMed](#)]
60. Gude, D.R.; Alvarez, S.E.; Paugh, S.W.; Mitra, P.; Yu, J.; Griffiths, R.; Barbour, S.E.; Milstien, S.; Spiegel, S. Apoptosis induces expression of sphingosine kinase 1 to release sphingosine-1-phosphate as a “come-and-get-me” signal. *FASEB J.* **2008**, *22*, 2629–2638. [[CrossRef](#)] [[PubMed](#)]
61. Liu, X.; Zeidan, Y.H.; Elojeimy, S.; Holman, D.H.; El-Zawahry, A.M.; Guo, G.W.; Bielawska, A.; Bielawski, J.; Szulc, Z.; Rubinchik, S.; et al. Involvement of sphingolipids in apoptin-induced cell killing. *Mol. Ther.* **2006**, *14*, 627–636. [[CrossRef](#)] [[PubMed](#)]
62. Shimabukuro, M.; Higa, M.; Zhou, Y.T.; Wang, M.Y.; Newgard, C.B.; Unger, R.H. Lipoapoptosis in beta-cells of obese prediabetic fa/fa rats. Role of serine palmitoyltransferase overexpression. *J. Biol. Chem.* **1998**, *273*, 32487–32490. [[CrossRef](#)] [[PubMed](#)]
63. Stunff, H.L.; Milstien, S.; Spiegel, S. Generation and metabolism of bioactive sphingosine-1-phosphate. *J. Cell. Biochem.* **2004**, *92*, 882–899. [[CrossRef](#)] [[PubMed](#)]
64. Becker, K.P.; Kitatani, K.; Idkowiak-Baldys, J.; Bielawski, J.; Hannun, Y.A. Selective Inhibition of Juxtannuclear Translocation of Protein Kinase C β II by a Negative Feedback Mechanism Involving Ceramide Formed from the Salvage Pathway. *J. Biol. Chem.* **2005**, *280*, 2606–2612. [[CrossRef](#)] [[PubMed](#)]
65. Nikolova-Karakashian, M.N.; Rozenova, K.A. Ceramide in Stress Response. *Adv. Exp. Med. Biol.* **2010**, *688*, 86–108. [[CrossRef](#)] [[PubMed](#)]
66. Chalfant, C.E.; Spiegel, S. Sphingosine 1-phosphate and ceramide 1-phosphate: Expanding roles in cell signaling. *J. Cell Sci.* **2005**, *118 Pt 20*, 4605–4612. [[CrossRef](#)]
67. Nelson, A.J.; Stephenson, D.J.; Bone, R.N.; Cardona, C.; Park, M.A.; Tusing, Y.G.; Lei, X.; Kokotos, G.; Graves, C.L.; Mathews, C.E.; et al. Lipid mediators and biomarkers associated with type 1 diabetes development. *JCI Insight* **2020**, *5*. [[CrossRef](#)]
68. Anderson, M.S.; Bluestone, J.A. The nod mouse: A Model of Immune Dysregulation. *Annu. Rev. Immunol.* **2005**, *23*, 447–485. [[CrossRef](#)]
69. Green-Mitchell, S.M.; Tersey, S.A.; Cole, B.K.; Ma, K.; Kuhn, N.S.; Cunningham, T.D.; Maybee, N.A.; Chakrabarti, S.K.; McDuffie, M.; Taylor-Fishwick, D.A.; et al. Deletion of 12/15-lipoxygenase alters macrophage and islet function in NOD-Alox15(null) mice, leading to protection against type 1 diabetes development. *PLoS ONE* **2013**, *8*, e56763.

70. Tersey, S.A.; Nishiki, Y.; Templin, A.T.; Cabrera, S.M.; Stull, N.D.; Colvin, S.C.; Evans-Molina, C.; Rickus, J.L.; Maier, B.; Mirmira, R.G. Islet beta-cell endoplasmic reticulum stress precedes the onset of type 1 diabetes in the nonobese diabetic mouse model. *Diabetes* **2012**, *61*, 818–827. [[CrossRef](#)]
71. Aoki, M.; Aoki, H.; Ramanathan, R.; Hait, N.C.; Takabe, K. Sphingosine-1-phosphate signaling in immune cells and inflammation: Roles and therapeutic potential. *Mediat. Inflamm.* **2016**, *2016*, 8606878.
72. Maceyka, M.; Milstien, S.; Spiegel, S. Sphingosine kinases, sphingosine-1-phosphate and sphingolipidomics. *Prostaglandins Other Lipid Mediat.* **2005**, *77*, 15–22. [[CrossRef](#)] [[PubMed](#)]
73. Pralhada Rao, R.; Vaidyanathan, N.; Rengasamy, M.; Mammen Oommen, A.; Somaiya, N.; Jagannath, M.R. Sphingolipid metabolic pathway: An overview of major roles played in human diseases. *J. Lipid.* **2013**, *2013*, 178910. [[CrossRef](#)]
74. Spiegel, S.; Milstien, S. Functions of the Multifaceted Family of Sphingosine Kinases and Some Close Relatives. *J. Biol. Chem.* **2007**, *282*, 2125–2129. [[CrossRef](#)]
75. Hait, N.C.; Oskeritzian, C.A.; Paugh, S.W.; Milstien, S.; Spiegel, S. Sphingosine kinases, sphingosine 1-phosphate, apoptosis and diseases. *Biochim. Biophys. Acta* **2006**, *1758*, 2016–2026. [[CrossRef](#)]
76. Taha, T.A.; Mullen, T.D.; Obeid, L.M. A house divided: Ceramide, sphingosine, and sphingosine-1-phosphate in programmed cell death. *Biochim. Biophys. Acta (BBA)—Biomembr.* **2006**, *1758*, 2027–2036. [[CrossRef](#)]
77. Taha, T.A.; Kitatani, K.; El-Alwani, M.; Bielawski, J.; Hannun, Y.A.; Obeid, L. Loss of sphingosine kinase-1 activates the intrinsic pathway of programmed cell death: Modulation of sphingolipid levels and the induction of apoptosis. *FASEB J.* **2005**, *20*, 482–484. [[CrossRef](#)]
78. Hu, W.; Xu, R.; Zhang, G.; Jin, J.; Szulc, Z.M.; Bielawski, J.; Hannun, Y.A.; Obeid, L.; Mao, C. Golgi Fragmentation Is Associated with Ceramide-induced Cellular Effects. *Mol. Biol. Cell* **2005**, *16*, 1555–1567. [[CrossRef](#)]
79. Hannun, Y.A.; Obeid, L.M. Many Ceramides. *J. Biol. Chem.* **2011**, *286*, 27855–27862. [[CrossRef](#)] [[PubMed](#)]
80. Kitatani, K.; Idkowiak-Baldys, J.; Hannun, Y.A. The sphingolipid salvage pathway in ceramide metabolism and signaling. *Cell. Signal.* **2008**, *20*, 1010–1018. [[CrossRef](#)] [[PubMed](#)]
81. Zhang, J.; Alter, N.; Reed, J.C.; Borner, C.; Obeid, L.; Hannun, Y.A. Bcl-2 interrupts the ceramide-mediated pathway of cell death. *Proc. Natl. Acad. Sci. USA* **1996**, *93*, 5325–5328. [[CrossRef](#)]
82. Song, H.; Bao, S.; Lei, X.; Jin, C.; Zhang, S.; Turk, J.; Ramanadham, S. Evidence for proteolytic processing and stimulated organelle redistribution of iPLA2b. *Biochim. Biophys. Acta (BBA)—Mol. Cell Biol. Lipids* **2010**, *1801*, 547–558.
83. Nozaki, J.I.; Kubota, H.; Yoshida, H.; Naitoh, M.; Goji, J.; Yoshinaga, T.; Mori, K.; Koizumi, A.; Nagata, K. The endoplasmic reticulum stress response is stimulated through the continuous activation of transcription factors ATF6 and XBP1 in *Inns2+*/Akitapancreatic β cells. *Genes Cells* **2004**, *9*, 261–270. [[CrossRef](#)] [[PubMed](#)]
84. Wijesinghe, D.S.; Allegood, J.C.; Gentile, L.B.; Fox, T.E.; Kester, M.; Chalfant, C.E. Use of high performance liquid chromatography-electrospray ionization-tandem mass spectrometry for the analysis of ceramide-1-phosphate levels. *J. Lipid Res.* **2010**, *51*, 641–651. [[CrossRef](#)] [[PubMed](#)]
85. Wang, G.; Bieberich, E. Sphingolipids in neurodegeneration (with focus on ceramide and S1P). *Adv. Biol. Regul.* **2018**, *70*, 51–64. [[CrossRef](#)] [[PubMed](#)]
86. Nganga, R.; Oleinik, N.; Ogretmen, B. Mechanisms of Ceramide-Dependent Cancer Cell Death. *Adv. Cancer Res.* **2018**, *140*, 1–25. [[CrossRef](#)]